Research Article | Vol. 26, No. 4 | 19 Feb 2018 | OPTICS EXPRESS 5043
Optics EXPRESS

Room-temperature electrically pumped InGaN-based microdisk laser grown on Si

MEIXIN FENG,[1,2] JUNLEI HE,[1,3] QIAN SUN,[1,2,3,*] HONGWEI GAO,[1,2] ZENGCHENG LI,[1] YU ZHOU,[1,2] JIANPING LIU,[1,3] SHUMING ZHANG,[1,3] DEYAO LI,[1] LIQUN ZHANG,[1] XIAOJUAN SUN,[4] DABING LI,[4] HUAIBING WANG,[1] MASAO IKEDA,[1] RONGXIN WANG,[1] AND HUI YANG[1,3]

[1]*Key Laboratory of Nano-devices and Applications, Suzhou Institute of Nano-Tech and Nano-Bionics, Chinese Academy of Sciences (CAS), Suzhou 215123, China*
[2]*Suzhou Institute of Nano-Tech and Nano-Bionics, CAS, Nanchang 330200, China*
[3]*School of Nano Technology and Nano Bionics, University of Science and Technology of China, Hefei 230026, China*
[4]*Changchun Institute of Optics Fine Mechanics and Physics, CAS, Changchun 130033, China*
[*]*qsun2011@sinano.ac.cn*

Abstract: Silicon photonics has been longing for an efficient on-chip light source that is electrically driven at room temperature. Microdisk laser featured with low-loss whispering gallery modes can emit directional lasing beam through a closely coupled on-chip waveguide efficiently, and hence is particularly suitable for photonics integration. The realization of electrically pumped III-nitride microdisk laser grown on Si has been impeded by the conventional undercut structure, poor material quality, and a limited quality of GaN microdisk formed by dry etching. Here we report a successful fabrication of room-temperature electrically pumped InGaN-based microdisk lasers grown on Si. A dramatic narrowing of the electroluminescence spectral line-width and a clear discontinuity in the slope of light output power plotted as a function of the injection current provide an unambiguous evidence of lasing. This is the first observation of electrically pumped lasing in InGaN-based microdisk lasers grown on Si at room temperature.

© 2018 Optical Society of America under the terms of the OSA Open Access Publishing Agreement

OCIS codes: (140.3948) Microcavity devices; (140.7300) Visible lasers; (130.3120) Integrated optics devices; (140.5960) Semiconductor lasers.

References and links

1. K. J. Vahala, "Optical microcavities," Nature **424**(6950), 839–846 (2003).
2. M. Hochberg and T. Baehr-Jones, "Towards fabless silicon photonics," Nat. Photonics **4**(8), 492–494 (2010).
3. S. Pimputkar, J. S. Speck, S. P. DenBaars, and S. Nakamura, "Prospects for LED lighting," Nat. Photonics **3**(4), 180–182 (2009).
4. Y. Mei, G. E. Weng, B. P. Zhang, J. P. Liu, W. Hofmann, L. Y. Ying, J. Y. Zhang, Z. C. Li, H. Yang, and H. C. Kuo, "Quantum dot vertical-cavity surface-emitting lasers covering the 'green gap'," Light Sci. Appl. **6**(1), e16199 (2017).
5. S. Masui, Y. Nakatsu, D. Kasahara, and S. Nagahama, "Recent Improvement in Nitride Lasers," Proc. SPIE **10104**, 101041H (2017).
6. A. C. Tamboli, E. D. Haberer, R. Sharma, K. Lee, S. Nakamura, and E. L. Hu, "Room-temperature continuous-wave lasing in GaN/InGaN microdisks," Nat. Photonics **1**(1), 61–64 (2007).
7. Y. H. Kim, S. H. Kwon, J. M. Lee, M. S. Hwang, J. H. Kang, W. I. Park, and H. G. Park, "Graphene-contact electrically driven microdisk lasers," Nat. Commun. **3**(1), 1123 (2012).
8. P. Miao, Z. Zhang, J. Sun, W. Walasik, S. Longhi, N. M. Litchinitser, and L. Feng, "Orbital angular momentum microlaser," Science **353**(6298), 464–467 (2016).
9. X. M. Lv, Y. Z. Huang, Y. D. Yang, L. X. Zou, H. Long, B. W. Liu, J. L. Xiao, and Y. Du, "Influences of carrier diffusion and radial mode field pattern on high speed characteristics for microring lasers," Appl. Phys. Lett. **104**(16), 161101 (2014).
10. Y. D. Yang, Y. Zhang, Y. Z. Huang, and A. W. Poon, "Direct-modulated waveguide-coupled microspiral disk lasers with spatially selective injection for on-chip optical interconnects," Opt. Express **22**(1), 824–838 (2014).
11. Y. Yang, B. Zhu, Z. Shi, J. Wang, X. Li, X. Gao, J. Yuan, Y. Li, Y. Jiang, and Y. Wang, "Multi-dimensional spatial light communication made with on-chip InGaN photonic integration," Opt. Mater. **64**(17), 160–165 (2017).

#318399 https://doi.org/10.1364/OE.26.005043
Journal © 2018 Received 27 Dec 2017; revised 9 Feb 2018; accepted 10 Feb 2018; published 16 Feb 2018

Optics EXPRESS

12. M. Feng, J. Wang, R. Zhou, Q. Sun, H. Gao, Y. Zhou, J. Liu, Y. Huang, S. Zhang, M. Ikeda, H. Wang, Y. Wang, and H. Yang, "On-chip integration of GaN-based laser, modulator, and photodetector grown on Si". (in review).
13. Y. C. Chi, Y. F. Huang, T. C. Wu, C. T. Tsai, L. Y. Chen, H. C. Kuo, and G. R. Lin, "Violet Laser Diode Enables Lighting Communication," Sci. Rep. **7**(1), 10469 (2017).
14. J. Sellés, V. Crepel, I. Roland, M. El Kurdi, X. Checoury, P. Boucaud, M. Mexis, M. Leroux, B. Damilano, S. Rennesson, F. Semond, B. Gayral, C. Brimont, and T. Guillet, "III-Nitride-on-silicon microdisk lasers from the blue to the deep ultra-violet," Appl. Phys. Lett. **109**(23), 231101 (2016).
15. M. Athanasiou, R. Smith, B. Liu, and T. Wang, "Room temperature continuous-wave green lasing from an InGaN microdisk on silicon," Sci. Rep. **4**(1), 7250 (2015).
16. H. W. Choi, K. N. Hui, P. T. Lai, P. Chen, X. H. Zhang, S. Tripathy, J. H. Teng, and S. J. Chua, "Lasing in GaN microdisks pivoted on Si," Appl. Phys. Lett. **89**(21), 211101 (2006).
17. S. Vicknesh, S. Tripathy, V. K. X. Lin, L. S. Wang, and S. J. Chua, "Fabrication of deeply undercut GaN-based microdisk structures on silicon platforms," Appl. Phys. Lett. **90**(7), 071906 (2007).
18. X. Liu, W. Fang, Y. Huang, X. H. Wu, S. T. Ho, H. Cao, and R. P. H. Chang, "Optically pumped ultraviolet microdisk laser on a silicon substrate," Appl. Phys. Lett. **84**(14), 2488–2490 (2004).
19. D. Visalli, M. V. Hove, M. Leys, J. Derluyn, E. Simoen, P. Srivastava, K. Geens, S. Degroote, M. Germain, A. P. D. Nguyen, A. Stesmans, and G. Borghs, "Investigation of Light-Induced Deep-Level Defect Activation at the AlN/Si Interface," Appl. Phys. Express **4**(9), 094101 (2011).
20. S. Nakamura, M. Senoh, S. Nagahama, N. Iwasa, T. Yamada, T. Matsushita, Y. Sugimoto, and H. Kiyoku, "High-power, long-lifetime InGaN multi-quantum-well structure laser diodes," Jpn. J. Appl. Phys. **36**(8B), L1059–L1061 (1997).
21. S. Nozaki, S. Yoshida, K. Yamanaka, O. Imafuji, S. Takigawa, T. Katayama, and T. Tanaka, "High-power and high-temperature operation of an InGaN laser over 3W at 85 °C using a novel double-heat-flow packaging technology," Jpn. J. Appl. Phys. **55**(4S), 04EH05 (2016).
22. Q. Sun, W. Yan, M. X. Feng, Z. C. Li, B. Feng, H. M. Zhao, and H. Yang, "GaN-on-Si Blue/White LEDs: Epitaxy, Chip, and Package," J. Semicond. **37**(4), 044006 (2016).
23. B. Leung, J. Han, and Q. Sun, "Strain relaxation and dislocation reduction in AlGaN step-graded buffer for crack-free GaN on Si (111)," Phys. Status Solidi., C Curr. Top. Solid State Phys. **11**(3-4), 437–441 (2014).
24. Y. Sun, K. Zhou, Q. Sun, J. P. Liu, M. X. Feng, Z. C. Li, Y. Zhou, L. Q. Zhang, D. Y. Li, S. M. Zhang, M. Ikeda, S. Liu, and H. Yang, "Room-temperature continuous-wave electrically injected InGaN-based laser directly grown on Si," Nat. Photonics **10**(9), 595–599 (2016).
25. D. Li, "GaN-on-Si laser diode: open up a new era of Si-based optical interconnections," Sci. Bull. **61**(22), 1723–1725 (2016).
26. S. Nakamura, "The roles of Structural Imperfections in InGaN-Based Blue Light-Emitting Diodes and Laser Diodes," Science **281**(5379), 956–961 (1998).
27. M. Ikeda, T. Mizuno, M. Takeya, S. Goto, S. Ikeda, T. Fujimoto, Y. Ohfuji, and T. Hashizu, "High-power GaN-based semiconductor lasers," Phys. Status Solidi, C Conf. Crit. Rev. **1**(6), 1461–1467 (2004).
28. L. Redaelli, M. Martens, J. Piprek, H. Wenzel, C. Netzel, A. Linke, Y. V. Flores, S. Einfeldt, M. Kneissl, and G. Tränkle, "Effect of ridge waveguide etch depth on laser threshold of InGaN MQW laser diodes," Proc. SPIE **8262**, 826219 (2012).
29. G. Yuan, K. Xiong, C. Zhang, Y. Li, and J. Han, "Optical Engineering of Modal Gain in a III-Nitride Laser with Nanoporous GaN," ACS Photonics **3**(9), 1604–1610 (2016).
30. C. Zhang, S. H. Park, D. Chen, D. W. Lin, W. Xiong, H. C. Kuo, C. F. Lin, H. Cao, and J. Han, "Mesoporous GaN for Photonic Engineering-Highly Reflective GaN Mirrors as an Example," ACS Photonics **2**(7), 980–986 (2015).
31. X. Zhang, Y. F. Cheung, Y. Zhang, and H. W. Choi, "Whispering-gallery mode lasing from optically free-standing InGaN microdisks," Opt. Lett. **39**(19), 5614–5617 (2014).
32. A. Pourhashemi, R. M. Farrell, D. A. Cohen, J. S. Speck, S. P. DenBaars, and S. Nakamura, "High-power blue laser diodes with indium tin oxide cladding on semipolar (20-21) GaN substrates," Appl. Phys. Lett. **106**(11), 111105 (2015).
33. X. Zhang, C. H. To, and H. W. Choi, "Optically-free-standing InGaN microdisks with metallic reflectors," Jpn. J. Appl. Phys. **56**(1S), 01AD04 (2017).
34. T. Nishida, H. Saito, and N. Kobayashi, "Efficient and high-power AlGaN-based ultraviolet light-emitting diode grown on bulk GaN," Appl. Phys. Lett. **79**(6), 711–712 (2001).
35. S. Nakamura, "InGaN/GaN/AlGaN-based laser diodes grown on epitaxially laterally overgrown GaN," J. Mater. Res. **14**(7), 2716–2731 (1999).

1. Introduction

Silicon based optoelectronic integrated circuit compatible with large-scale low-cost fabrication technology is deemed as a promising path to overcome the fundamental limits of communication and computation technologies in speed and bandwidth [1,2]. However, Si with an indirect band structure cannot be adopted as an efficient light emitter. III-nitride semiconductors with a direct band structure have been widely used for efficient light emitting

Optics EXPRESS

diodes and laser diodes (LDs) with a huge commercial success [3–5]. Microdisk lasers featured with low-loss and high-quality whispering gallery modes (WGMs) hold a great potential for an ultralow threshold [1,6–8]. And they have smaller footprint, lower power consumption, and better high-speed modulation characteristics, as compared with Fabry–Pérot cavity lasers [9]. Therefore microdisk lasers are expected to be a key component in densely integrated photonic circuits. Moreover, microdisk laser can emit directional lasing beam through a closely coupled waveguide directly and efficiently, which is of great benefits to on-chip integration [10]. Therefore, III-nitride semiconductor microdisk lasers on Si may serve as an alternative on-chip light source for Si based optoelectronic integration with III-nitride waveguide. Additionally, they can be also used for photonic integration in the ultraviolet and visible light range and visible light communication [11–13].

Room-temperature electrically pumped InGaN-based microdisk laser grown on Si has been pursued for over a decade [14–18]. It is mainly limited by the conventional undercut structure, poor material quality, and a limited quality of GaN microdisk. To our best knowledge, only optically pumped lasing in III-nitride microdisk grown on Si has been achieved, which is very complicated for on-chip integration. Here, we report a demonstration of room-temperature electrically pumped InGaN-based microdisk lasers grown on Si.

2. Experiments

In the previous studies, a ‘mushroom-like’ architecture featured with an undercut structure was commonly used to enhance the optical confinement along the vertical direction, as shown in Fig. 1(a) [14–18]. However, this kind of ‘mushroom-like’ architecture has several drawbacks. Firstly, Si underneath the InGaN-based microdisk was often partially removed to form an undercut, and electrical current injection must be through the Si substrate. However, the 370-nm-thick undoped AlN (with a large bandgap of 6.2 eV) and nearly 700-nm-thick undoped AlGaN layer buffer between the Si substrate and the active region is highly resistive. Hence, it is very difficult for current injection into the peripheral region of the ‘mushroom-like’ InGaN microdisk lasers with an undercut structure even though a conductive path existed at the AlN/Si interface [19]. Secondly, the AlN buffer with a high dislocation density (typically 10^{10}-10^{11} cm^{-2}) is within the optical cavity, which will induce optical loss and hence increase the threshold current [14–18]. Thirdly, when the Si underneath the periphery is etched away, the heat generated at the periphery cannot dissipate directly to the Si substrate. The resulted high junction temperature would affect the device performance and reliability [20,21]. In addition, the ‘mushroom-like’ microdisk structure is mechanically supported only by the thin pivot in the center, and hence is not robust, easy to be broken. Lastly, the fabrication process of InGaN-based microdisk lasers with an undercut structure is very complicated, and the size of the pivots underneath is hard to control, which would influence the uniformity, yield, and reproducibility of InGaN microdisk lasers on Si.

Optics EXPRESS

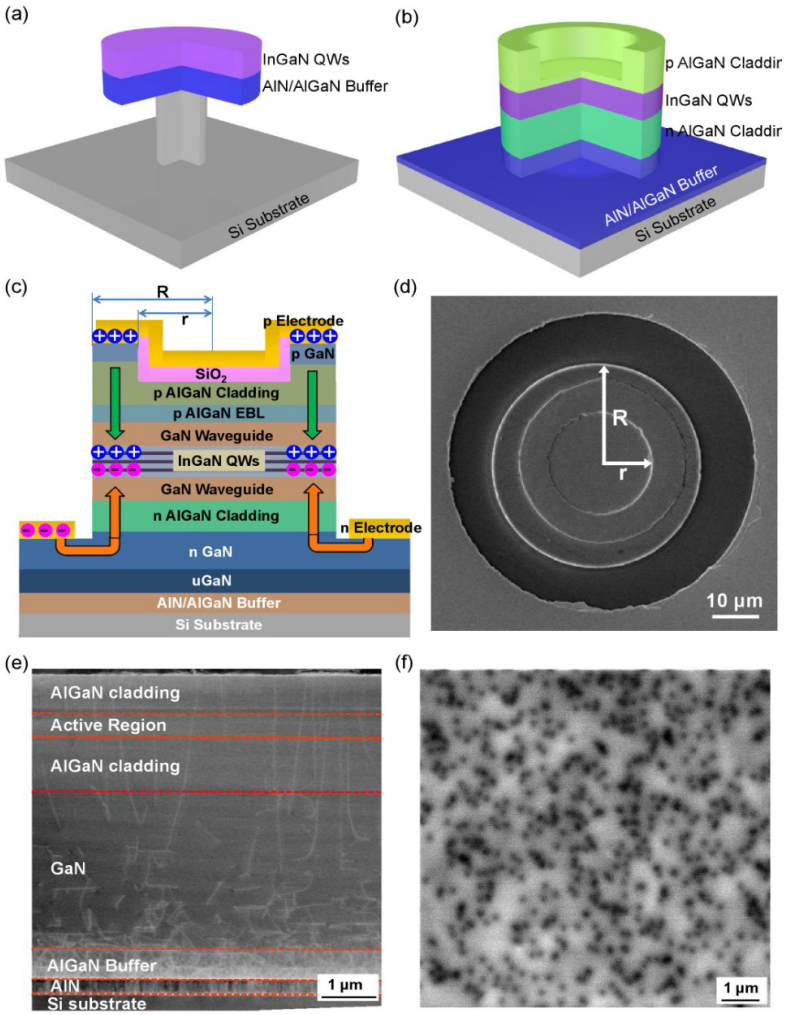

Fig. 1. The schematic architectures of the reported 'mushroom-like' InGaN-based microdisk laser on Si with an undercut structure (a) and a 'sandwich-like' InGaN microring laser grown on Si with AlGaN cladding layers (b). (c) The detailed schematic structure of InGaN microring laser grown on Si with AlGaN cladding layers. *R* and *r* are the radiuses of the outer and inner circles, respectively. The 5.8-μm-thick laser epitaxial structure consisted of a 370-nm-thick AlN nucleation layer, Al composition step-graded AlGaN multi-layers consisting of a 280-nm-thick $Al_{0.35}Ga_{0.65}N$ layer and a 415-nm-thick $Al_{0.17}Ga_{0.83}N$ layer, a 1-μm-thick undoped GaN layer, a 1.6-μm-thick n-type GaN layer, a 1.3-μm-thick n-type $Al_{0.07}Ga_{0.93}N$ cladding layer, a 80-nm-thick n-type GaN lower waveguide layer, three pairs of 2.5-nm-thick undoped $In_{0.1}Ga_{0.9}N$ quantum wells (QWs) and 7.5-nm-thick undoped $In_{0.02}Ga_{0.98}N$ quantum barrier layers, a 60-nm-thick undoped GaN upper waveguide layer, a 20-nm-thick p-type $Al_{0.2}Ga_{0.8}N$ electron blocking layer (EBL), 100 pairs of 3-nm-thick p-type $Al_{0.11}Ga_{0.89}N$ and 3-nm-thick p-type GaN superlattice (SL) cladding layers, and a 30-nm-thick p-type GaN contact layer. The device was fabricated in a co-planar structure, with both p- and n-contact pads at the same side. (d) Scanning electron microscope image of one as-fabricated InGaN microring laser grown on Si (R = 20 μm and r = 10 μm). (e) Cross-sectional high-angle annular dark-field scanning transmission electron microscope (STEM) image of an InGaN-based microdisk laser structure grown on Si. The total thickness of the entire epitaxial structure was 5.8 μm. (f) Panchromatic cathodoluminescence image of the GaN film grown on Si. The density of threading dislocations (TDs) in the GaN film represented by the dark spots was about 6×10^8 cm^{-2}.

Here, we adopted a 'sandwich-like' architecture with both upper and lower AlGaN cladding layers to confine the optical field in InGaN-based microdisk lasers grown on Si, as

Optics EXPRESS

shown in Fig. 1(b). The AlGaN cladding layers have a lower refractive index than GaN, and hence can be used to confine the optical field from the top and the bottom directions. To avoid the optical field leaking into the highly defective AlN/AlGaN buffer layers and reduce optical loss, 1.3-μm-thick n-type AlGaN cladding layer was grown to confine most of the optical field in the high-quality GaN waveguide layers and the active region. Besides the optical confinement, the lower n-type AlGaN cladding layer could also facilitate heat dissipation to the substrate. According to our calculation result, the thermal resistance of the 'sandwich-like' microdisk laser with AlGaN cladding layers on Si is only 5% of that of the 'mushroom-like' microdisk laser with an undercut structure. This remarkable difference in thermal resistance would have a significant impact on the realization of electrically pumped InGaN-base microdisk laser on Si. For this 'sandwich-like' structure, the n electrode could be deposited on the n-type GaN contact layer, and the electrons can be easily injected through the n-type AlGaN lower cladding layer into the active region [Fig. 1(c)], with a limited electrical resistance. Figure 1(d) shows the SEM image of an as-fabricated InGaN microring laser on Si. Compared with the 'mushroom-like' InGaN microdisk lasers with an undercut structure, this 'sandwich-like' structure is very robust with a fully mechanical support from the underlying n-type AlGaN cladding layer, and the fabrication process is much simpler and more controllable.

As compared with the conventional 'mushroom-like' structure, however, the 'sandwich-like' microdisk laser structure requires an epitaxial growth of a much thicker stack on Si. To obtain a crack-free high-quality InGaN-based microdisk laser structure grown on Si, the 17% mismatch in lattice constant and the 54% misfit in thermal expansion coefficient (CTE) between GaN and Si have to be overcome [22–25]. The lattice mismatch usually causes a high density (10^{10}–10^{11} cm^{-2}) of TDs, affecting the internal quantum efficiency and the device performance [26,27]. The CTE misfit normally results in a high tensile stress, wafer bowing, and even formation of microcrack networks during the cooling down from the growth temperature to room temperature [22–25]. And the thick AlGaN cladding layers grown on GaN would add extra tensile stress in the epitaxial film. Therefore, stress control and defect reduction are crucial to the realization of the 'sandwich-like' microdisk laser on Si.

To tackle with these challenges, an Al-composition step-graded AlN/AlGaN/ multilayer buffer was inserted between GaN film and Si substrate to accumulate enough compressive strain, which cannot only compensate the tensile stress due to CTE mismatch during the cooling down, but also make TDs incline, interact and even annihilate with each other [22–25]. According to the cross-sectional high-angle annular dark-field STEM observation [Fig. 1(e)], a substantial portion of TDs were filtered out from the AlN nucleation layer to the GaN thick layer. The as-grown GaN film on Si showed a defect density of ~6×10^8 cm^{-2} [Fig. 1(f)]. On top of the high-quality GaN template grown on Si, InGaN QW active region was overgrown and sandwiched by GaN waveguide and AlGaN cladding layers [Figs. 1(c) and 1(e)]. The entire epitaxial stack [Fig. 1(e)] of the InGaN-based microdisk laser structure was about 5.8 μm thick, yet with a very short length (~0.5 mm) of edge cracks.

In order to realize room temperature electrically pumped InGaN-based microdisk laser on Si, it is indispensible to fabricate a well defined microdisk with a high quality. The quality of microdisk is mainly determined by its shape and sidewall quality. Because WGMs are normally concentrated very close to the periphery of microdisk, its sidewall roughness and defects can induce a strong optical loss, resulting in a low quality. Since there is no chemical solution that can effectively etch *c*-plane Ga-polar GaN, dry etching was commonly utilized to pattern InGaN-based circular microdisk. A nickel hard mask, instead of a photoresist mask, was taken to reduce mask erosion during the dry etching process and maintain the circular shape of the microdisk. Tetramethyl ammonium hydroxide (TMAH) wet etching treatment was performed to remove the dry-etching induced damage and smooth the sidewall, which effectively reduced the non-radiative recombination centers and the optical loss. Figures 2(a) and 2(b) shows the SEM images of the sidewalls and the threshold currents of InGaN-based

Optics EXPRESS

microring lasers (R = 100 μm and r = 90 μm) before and after the TMAH wet etching treatment. Right after the dry etching (but before the TMAH wet etching treatment), the microdisk sidewall was quite rough [Fig. 2(a)]. The sidewall became much smoother [Fig. 2(b)] after the TMAH wet etching treatment. And the threshold current of the as-fabricated InGaN-based microring lasers decreased from nearly 1500 to 1000 mA [Fig. 2(c)], confirming that the microdisk sidewall quality was significantly improved by the TMAH wet chemical polishing.

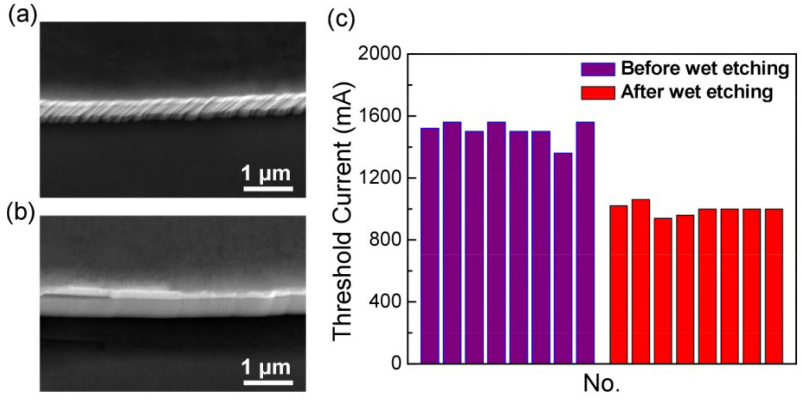

Fig. 2. (a), (b), SEM images of microdisk sidewall before (a) and after (b) TMAH wet etching. (c) Threshold currents of InGaN-based microring lasers grown on Si (R = 100 μm and r = 90 μm) before and after the TMAH wet etching treatment.

Microdisk resonator is one of the most commonly used microdisk structures. And the WGMs are usually concentrated very close to the periphery of the microdisk. To achieve an electrically pumped microdisk laser, current injection far away from the periphery of the microdisk not only has little contribution to the WGMs, but also generates lots of heat within the microdisk. Therefore, the undesired current injection into the central region of the microdisk would increase the junction temperature and affect the threshold current. To attack this problem, microring resonator [Figs. 1(b), 1(c), and 1(d)] was adopted in this study. The p-AlGaN/GaN SL upper cladding layer in the inner circle was partially removed to enhance the optical confinement in the lateral direction, and SiO_2 was deposited to block hole injection into the inner circle. Compared with the conventional microdisk resonators, microring resonators have more compact cavity volume and better high-speed modulation characteristics due to less effect of carrier space hole-burning and diffusion [9].

3. Results and dscussion

The electroluminescence (EL) characteristics of an as-fabricated InGaN-based microring laser grown on Si (R = 20 μm and r = 10 μm) were measured under a pulsed electrical injection at room temperature (Fig. 3). Thanks to the use of nickel hard mask, the circularity of the microring was well preserved, which was confirmed by the circular spontaneous emission pattern, as shown in the inset of Fig. 3(a). As the injection current was increased from 50 to 250 mA, the full width at half maximum (FWHM) of the emission spectrum quickly narrowed down to 0.4 nm [Fig. 3(b)], and the microring laser emits with a peak wavelength of 412.4 nm [Fig. 3(a)]. Also, the EL light output power increased quickly with the injection current. The plot of the light output power as a function of the pulsed injection current exhibited a distinct turning point at the lasing threshold current of 250 mA [Fig. 3(c)]. The statistical results (Fig. 4) regarding the threshold current for the as-fabricated InGaN-based microring lasers grown on Si indicate a decent yield and reproducibility of the process.

Optics EXPRESS

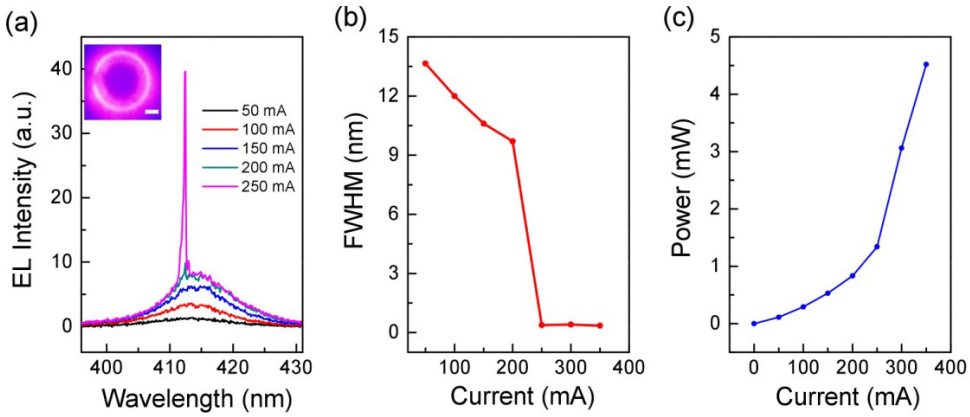

Fig. 3. (a) EL spectra of an as-fabricated InGaN-based microring laser grown on Si (R = 20 μm and r = 10 μm) measured under various pulsed currents. The inset showed a top-view emission pattern of the device at a pulsed injection current of 200 mA (below the lasing threshold), and the scale bar was 10 μm. The left-side segment of the circular emission pattern was blocked by the electrical probe. (b) FWHM of the EL spectra as a function of the pulsed injection current. (c) EL light output power as a function of the injection current. Only part of the light output was collected from the edge of the microring laser under a pulsed injection current at room temperature. The electrical pumping pulse width was 400 ns, and the repetition rate 10 kHz.

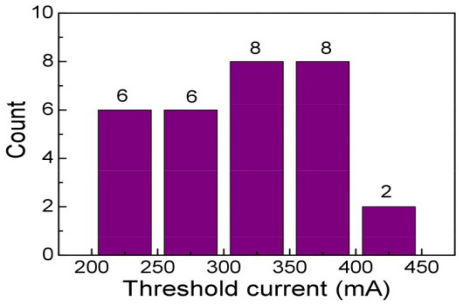

Statistic results

	Minimum	Average	Medium
I_{th} (mA)	240	344	340
J_{th} (kA/cm²)	25.5	36.5	36.1

Fig. 4. The threshold current distribution of 30 microring lasers grown on Si (R = 20 μm and r = 10 μm). All the measurements were taken under a pulsed injection current at room temperature. The electrical pumping pulse width was 400 ns and the repetition rate 10 kHz.

Figure 5 compared the EL light output power of an InGaN-based microring laser and a microdisk laser grown on Si before the TMAH wet etching treatment. The threshold current of the InGaN-based microring laser (R = 50 μm and r = 40 μm) was about 800 mA. In contrast, the threshold current of the same size InGaN microdisk laser (R = 50 μm and r = 0 μm) was about 1600 mA, which was twice of that of the InGaN microring laser. The injected current in the central region of the microdisk laser (away from the periphery) contributed little to the WGMs, but generated undesired heat, elevating the junction temperature. Therefore, the microdisk laser had both a much higher threshold current and smaller slope efficiency than the microring laser of same size. This experimental observation confirmed that the current blocking layer in the microring structure was crucial for the device performance improvement of InGaN-based electrically pumped microdisk lasers.

Optics EXPRESS

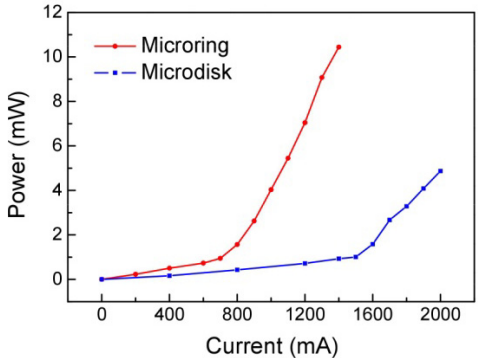

Fig. 5. Peak light output power of InGaN-based microring laser (R = 50 μm and r = 40 μm) and microdisk laser (R = 50 μm and r = 0 μm) grown on Si measured under various pulsed currents at room temperature. The electrical pumping pulse width was 400 ns, and the repetition rate 10 kHz.

For the convenience of electrical contact probing, the smallest radius of InGaN microdisk laser in this study was currently set as 20 μm. By shrinking the microdisk diameter by one or two orders of magnitude, the threshold current is expected to drop significantly. Besides the influence of microdisk size, the relatively high threshold current of the as-fabricated microring laser was also related to the relatively weak optical confinement and the relatively high TD density. According to the calculation results, the vertical optical confinement in the QWs for the as-fabricated structure with AlGaN cladding layers was only 1.84% (Fig. 6). The relatively weak optical confinement along the vertical direction led to some optical leakage and an increase in threshold current [28,29]. Several literatures reported that the optical confinement can be enhanced by nanoporous GaN [29,30], indium tin oxide (ITO) [31,32] or Ag mirror [33]. On the other hand, TDs often cause a significant portion of the injected carriers to recombine non-radiatively [34], which affects the internal quantum efficiency and elevates the junction temperature and the threshold current of InGaN-based microdisk lasers. Previous reports showed that the TD density of GaN can be reduced from 10^8 down to 10^6 cm^{-2} through epitaxial lateral overgrowth [26,35]. A study of epitaxial lateral overgrowth of GaN on Si and small-size microdisk lasers with nanoporous GaN, ITO or Ag based cladding layers is underway to improve the performance of InGaN-based microdisk lasers grown on Si.

4. Conclusion

InGaN-based ‘sandwich-like’ microdisk laser has been successfully grown on Si, and fabricated with a decent quality by the wet chemical polishing of the dry-etched microdisk sidewall. A dramatic narrowing of the EL spectral line-width and a clear discontinuity in the slope of the EL light output power plotted as a function of the injection current for the as-fabricated InGaN-based microring laser provided an unambiguous evidence of lasing. This is the first observation of room-temperature electrically pumped lasing in InGaN-based microdisk laser diode grown on Si.

Appendix

A.1 Optical field distribution of the as-fabricated microring lasers grown on Si

The schematic architecture of the as-fabricated ‘sandwich-like’ InGaN-based microring laser grown on Si with AlGaN cladding layers (CLs) is shown in Fig. 1(c). We calculated the optical field distribution of the ‘sandwich-like’ structure, as shown in Fig. 6. The optical confinement in the QWs was only 1.84%.

Optics EXPRESS

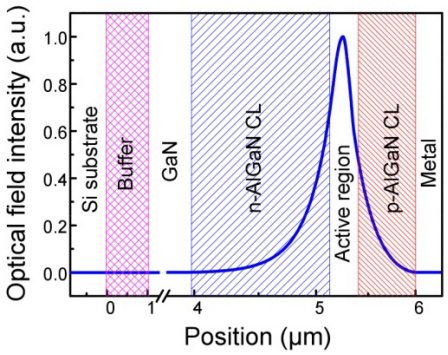

Fig. 6. The optical field distribution of the as-fabricated 'sandwich-like' InGaN-based microring laser grown on Si with AlGaN CLs.

Funding

National Key R & D Program (2017YFB0403100,2017YFB0403101); National Natural Science Foundation of China (NSFC) (61534007, 61404156, 61522407, 61604168, 61775230); Key Frontier Scientific Research Program of the Chinese Academy of Sciences (QYZDB-SSW-JSC014); Science and Technology Service Network Initiative of the Chinese Academy of Sciences; Key R & D Program of Jiangsu Province (BE2017079); Natural Science Foundation of Jiangsu Province (BK20160401); China Postdoctoral Science Foundation (2016M591944); Open fund of the State Key Laboratory of Luminescence and Applications (SKLA-2016-01); Open fund of the State Key Laboratory of Integrated Optoelectronics (IOSKL2016KF04, IOSKL2016KF07); Seed fund from SINANO, CAS (Y5AAQ51001).

Acknowledgment

The authors are thankful for the technical support from Nano Fabrication Facility, Platform for Characterization & Test, Nano-X of SINANO, CAS, and Prof. Qin Chen's valuable discussion.

159.226.165.17 {ts '2019-08-09 02:10:57'}